Journal of Clinical Toxicology
ISSN: 2161-0495

Wan et al., J Clin Toxicol 2019, 9:1
DOI: 10.4172/2161-0495.1000403

Research Article Open Access

First-Principles Calculations of the Adsorption Property of C_6H_7N and C_7H_9N on Pd-doped TiO_2 Anatase (1 0 1)

Yingang Gui[1], **Qianqian Wan**[2*] **and Ling Luo**[3]

[1]*College of Engineering and Technology, Southwest University, China*

[2]*Department of Endocrinology, Zhongnan Hospital of Wuhan University, China*

[3]*Chongqing University Cancer Hospital & Chongqing Cancer Institute & Chongqing Cancer Hospital, China*

[*]**Corresponding author:** Qianqian Wan, College of Engineering and Technology, Southwest University, China, E-mail: wanqq@whu.edu.cn

Received date: December 13, 2018; **Accepted date:** December 27, 2018; **Published date:** January 03, 2019

Abstract

In this work, we proposed a novel Pd-doped TiO_2 anatase (1 0 1), material as the gas sensing material to detect typical lung cancer volatile organic compounds: aniline (C_6H_7N) and *o*-toluidine (C_7H_9N). After analyse the adsorption structure, charge transfer, the density of states and band structure, it is found that Pd-TiO_2 presents good gas sensing properties to C_6H_7N and C_7H_9N. The single doped Pd atom acts as the active site to interact with the gas molecules, which causes the electron redistribution and the change of conductivity of adsorption system. According to the different change characteristics of conductivity upon different gas molecules adsorption, Pd-TiO_2 material can not only realize high gas sensitivity, but also realizes selectivity to C_6H_7N and C_7H_9N. The calculation results play a guiding role to prepare high-performance Pd-TiO_2 material gas sensor in experiment.

Keywords: Lung cancer; Volatile organic compounds; Pd doping; TiO_2 anatase (1 0 1); DFT method

Introduction

Lung cancer, as a kind of therioma, has been one of the most serious diseases that threat human life in the world today [1,2]. Influenced by smoking, carcinogen, hazardous air pollutants [3-6], the incidence and mortality of lung cancer are experiencing explosive growth in recent years. According to recent statistics [7-9], both the incidences and mortality of lung cancer for male rank first among all of the therioma. Though the incidence and mortality of lung cancer for female are less than that of male [10], they still ranked in the front. It is urgent to find effective methods to reduce the incidence and mortality. Generally, the patients go to hospital and get formal treatment only after they realize they have already get lung cancer [11,12]. Sometimes it has been got really serious, making them miss the important time to get immediate treatment at early stage. Therefore, developing a portable lung cancer detection device for early prevention and detection can be an optimal method to realize reduce the incidence and mortality, which possesses high-efficiency, flexibility, safety and low-cost with enough detection precision.

There will be lots of symptoms occur along with the occurrence of lung cancer at early stage, such as lung pain, cough and hemoptysis [13]. Based on these symptoms it is feasible to find the effective methods to detect the lung cancer. According to recent studies, the volatile organic compounds of lung cancer patients contain specific gas molecules that can be used to characterize the type and severity of lung cancer [14,15]. However, it is nearly impossible to detect the type and concentration of all volatile organic compounds molecules at the same time. In this study, we chose aniline (C_6H_7N) and *o*-toluidine (C_7H_9N) as the typical gas molecules to characterize lung cancer due to its universality and high concentration compared with other volatile organic compounds [16].

Due to the high sensitivity, fast repose and flexibility of gas sensors, it has been widely applied in industrial manufacture, environmental monitoring and gas detection[17,18]. While until now, there are no existing sensors that used to detect C_6H_7N and C_7H_9N, nor any studied reported about developing these gas sensors. In order to realize the high-precision detection, it is urgent to studies new gas sensor based on novel gas sensing materials. TiO_2 anatase, a kind of n-type metal transition metal oxide gas sensing material, has attracted widespread attention because of its advantages in low work temperature, low-cost, easy preparation and high stability [19,20]. In this study, TiO_2 anatase (1 0 1), abbreviated to TiO_2, is proposed as the gas sensing material to analyse its adsorption properties and gas sensing mechanism to C_6H_7N and C_7H_9N based on first principle calculations. In addition, Pd single metal doping method has been adopted to enhance its gas sensitivity according to previous research [21-23].

Methods

All of first-principles calculations are carried out on Dmol^3 module of Materials Studio, which has been widely used to analyse and predict the properties of materials [24]. First, Pd-TiO_2 (1 0 1), abbreviated to Pd-TiO_2, was built and optimized by substituting one Ti atom with Pd atom on surface. A periodic boundary model with lattice parameters 10.89 Å × 11.33 Å × 19.35 Å was adopted in our work, which is sufficient to avoid the interaction between adjacent gas adsorption structures [25]. Then C_6H_7N and C_7H_9N molecules were built and optimized to reach their most stable structures. Finally, C_6H_7N and C_7H_9N molecules are separately relaxed onto the surface of Pd-TiO_2. In order to ensure the computation accuracy, various approaching manners of C_6H_7N and C_7H_9N molecules were considered to find the lowest energy structures.

The geometry optimization was calculated by Generalized Gradient Approximation (GGA) with Perdew-Burke-Ernzerhof (PBE) [26],

which possessed high accuracy on calculating the electron-electron exchange and correlation interactions. Spin-polarized density functional theory was applied to deal with the electronic properties calculations of adsorption structures. The calculation parameters of electronic core treatment and basis set were all electrons and Double Numerical plus D-Functions (DND). In order to ensure calculation accuracy, the energy threshold, maximum force and self-consistent field convergence criteria were set as 5.44×10^{-4} eV, 1.09×10^{-1} eV/Å and 2.72×10^{-4} eV, respectively. Moreover, The Brillouin zone integrations are performed using a $1 \times 1 \times 1$ Monkhorst-Pack mesh in calculations, which is shown to be a good approximation for Pd-TiO_2 [27].

When gas molecules interact with the surface of Pd-TiO_2, the interaction energy was defined as adsorption energy (E_{ads}), which can be calculated from following equation (1):

$$E_{ads} = E_{surface/gas} - E_{surface} - E_{gas} \quad (1)$$

$E_{surface/gas}$ represents the total energy after gas molecules adsorbed on the surface of Pd-TiO_2. $E_{surface}$ represents the total energy of Pd-TiO_2 after reaching the lowest energy status. E_{gas} is the total energy of isolated gas molecules before adsorption. If $E_{ads}<0$, the adsorption process is assumed to be exothermic and generally occurs spontaneously.

The electrons redistribute during the gas molecules adsorption process, which directly influence the conductivity of the adsorption system. And Mulliken population analysis is used to assess charge density distribution [28,29]. Then the charge transfer (Q_T) between gas molecule and surface is calculated using the following equation (2), where $Q_{adsorbed\ gas}$ and $Q_{isolate\ gas}$ represent the total carried charge of gas molecules after and before adsorption on the surface of Pd-TiO_2,

$$Q_T = Q_{adsorbed\ gas} - Q_{isolate\ gas} \quad (2)$$

Results and Discussion

The structural parameters of Pd-TiO_2, C_6H_7N and C_7H_9N

In order to make the geometric structures of Pd-TiO_2, C_6H_7N and C_7H_9N meet the experimental results, we have obtained the lowest energy structures through DFT methods as shown in Figure 1. On the surface of perfect TiO_2 before Pd Doping, there are two types of oxygen atoms, that is O_{2c} (with two coordinate bonds) and O_{3c} (with two coordinate bonds). Similarly, two types of Ti atoms exist on the surface, that is Ti_{5c} (with five coordinate bonds) and Ti_{6c} (with six coordinate bonds). According to study in this work and other researches, the site between two O_{2c} is the most probable site for single Pd atom doping because it reaches the lowest energy and most stable structure. The Pd atom is obviously protrude out of the surface TiO_2 with a distance of Pd-oxygen 2.24 Å due to the great radius of Pd atom. The protruding structure of Pd atom acts as an active site to adsorb gas molecules because of its unsaturated bond. The structure of C_6H_7N is formed by substituting a hydrogen atom with one amidogen on the benzene ring as shown in Figure 1 (A). The bond distances of N-H and N-C are 1.02 Å and 1.40 Å, respectively. And angles of H-N-H and H-N-C are 111.6 degree and 114.5 degree, respectively. For C_7H_9N molecule, two adjacent hydrogen atoms on benzene ring are replaced by an amidogen and a methyl. The bond distances and angles of amidogen in C_7H_9N are almost the same with that of C_6H_7N molecule. The bond distances of C-H and C-C in methyl is 1.11 Å and 1.50 Å, respectively. And the corresponding bond angles are 106.9 degree and 110.9 degree are 1.02 Å and 1.40 Å, respectively.

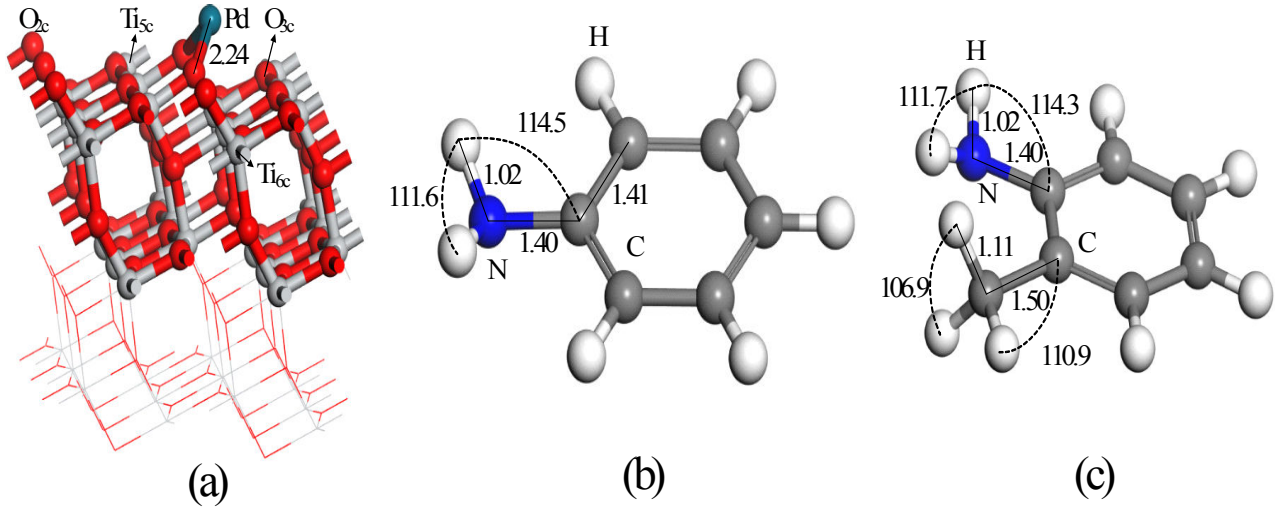

Figure 1: The optimized structures: (a) Pd-TiO_2, (b) C_6H_7N and (c) C_7H_9N. The unit of bond length and angle is Å and degree, respectively.

The adsorption structural parameters of C_6H_7N and C_7H_9N on the surface Pd-TiO_2

In order to ensure the computation accuracy, various approaching manners of C_6H_7N and C_7H_9N molecules were considered to find the lowest energy structures. Figure 2 and Table 1 shows the adsorption structural parameters of C_6H_7N adsorbed Pd-TiO_2 (C_6H_7N/Pd-TiO_2) and C_7H_9N adsorbed Pd-TiO_2 (C_7H_9N/Pd-TiO_2).

C_6H_7N molecule prefers to interact on the surface of Pd-TiO_2 through the physisorption between Pd atom and N atom because of their polyvalency property. The interaction distance is 2.20 Å. Due to the activity of Pd atom, the Eads for C_6H_7N adsorption has reached -1.40 eV. The great E_{ads} provides the prerequisite to detect C_6H_7N gas

in the volatile organic compounds. There are only 0.20 electron transfers from C_6H_7N molecule to Pd-TiO_2. The gas molecule adsorption has no induced the structural change of C_6H_7N molecule and Pd-TiO_2.

C_7H_9N molecule tends to interact with Pd-TiO_2 by hydrogen of the benzene ring. The adsorption distance is 2.83 Å when the adsorption system reaches the lowest energy, which is apparently larger than that of C_7H_9N/Pd-TiO_2. In addition, the E_{ads} is distinctly less than the adsorption energy of C_7H_9N/Pd-TiO_2. The charge transfer from one C_7H_9N to Pd-TiO_2 is 0.23 e. We conclude that the C_7H_9N is physically adsorbed on the surface of Pd-TiO_2.

System	Structure	d_1 (Å)	E_{ads} (eV)	Q_T (e)
C_6H_7N/Pd-TiO_2	-N	2.2	-1.4	0.2
C_7H_9N/Pd-TiO_2	-H	2.83	-0.25	0.23

Table 1: Adsorption energy (E_{ads}), charge transfer (Q_T), and the binding distance from the gases to Ni atom.

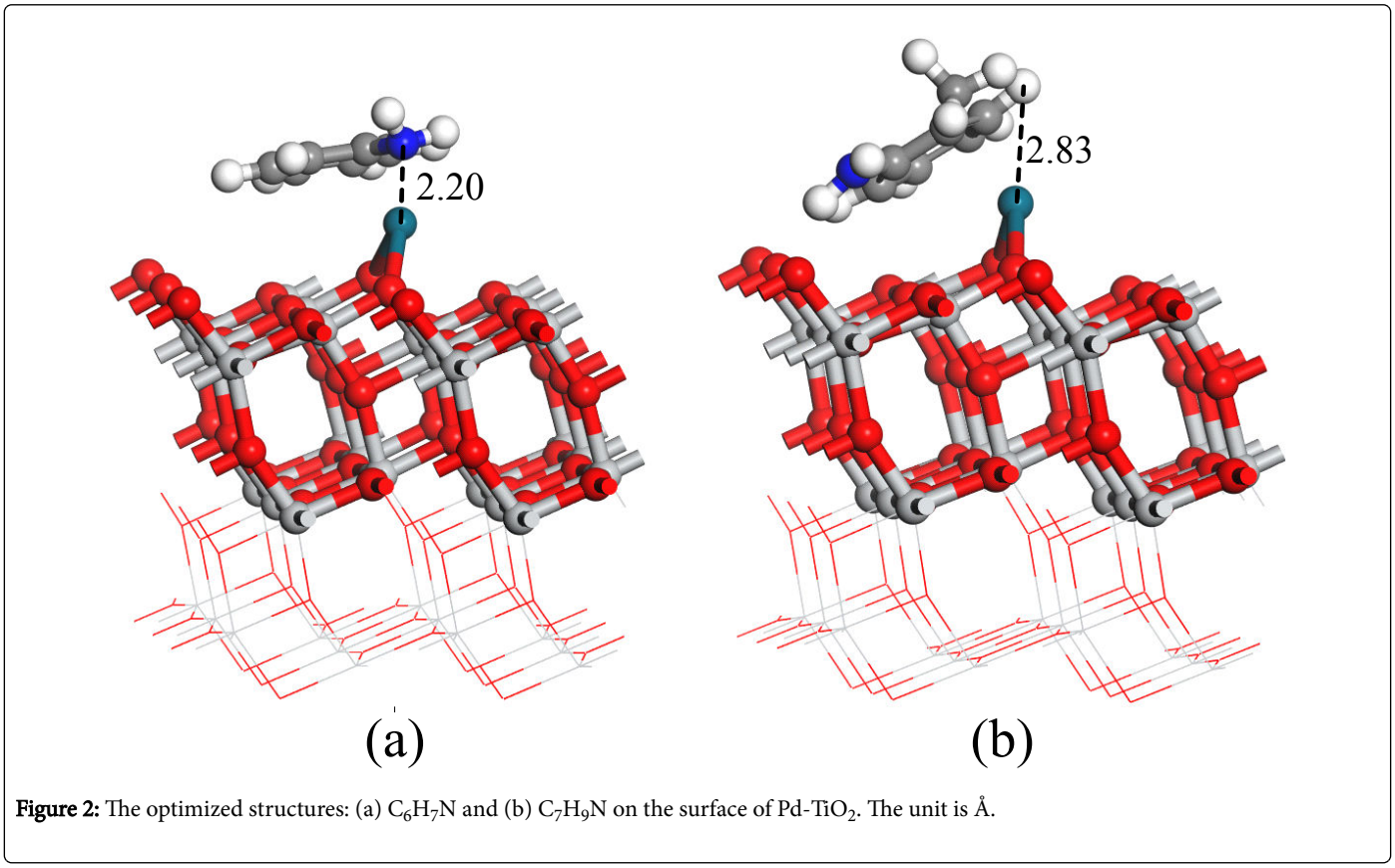

Figure 2: The optimized structures: (a) C_6H_7N and (b) C_7H_9N on the surface of Pd-TiO_2. The unit is Å.

The electronic property analysis of adsorption systems

To detect the type and concentration of C_6H_7N and C_7H_9N in volatile organic compounds molecules of lung cancer patients, it is necessary to analyse the electronic property analysis of adsorption systems. Basing on the gas detection mechanism of metal oxide resistance-type gas sensor, the Total Density of States (TDOS), Partial Density of States (PDOS), band structure and molecular orbital are calculated by DFT method to analyse the conductivity change of the gas molecules adsorption system.

Figure 3(a) shows the TDOS of adsorption system and PDOS of adsorbed molecules. The Fermi level is located at 0 eV. The TDOS of TiO_2 is discontinuous range -2~-1 eV, verifying the its semiconductor property. When one C6H7N molecule adsorbs on the surface of Pd-TiO_2, the TDOS becomes continuous in the entire range of energy. Except the distinct decrease of TDOS range -1~0 eV, TDOS tends to increase at other energy range. Part of the contribution of increased TDOS comes from the PDOS of C_6H_7N molecule during the adsorption process as show in Figure 3(b). Comparing with the TDOS of C_6H_7N adsorption system, Though the change of TDOS for C_7H_9N is similar to that of C_6H_7N adsorption, but the increment of TDOS range -2~0 eV is obviously larger as shown in Figure 3(c). The PDOS of adsorbed C_7H_9N molecule also makes great contribution to the increased TDOS C_7H_9N adsorption system as can be seen in Figure 3(d). According to the increase of TDOS during C_6H_7N and C_7H_9N adsorption, we conclude that both of the lung cancer volatile organic compounds increase the conductivity of adsorption system.

Band structure reflects directly the electron filling at different energy level. Figure 4 shows the band structure of Pd-TiO_2 and gas adsorbed Pd-TiO_2. As can been seen in Figure 4(a), Electronic forbidden band exists in valence band rang -2~-1 eV, which limit the transition of electron from valence band to conduction band. According to other related study about the band structure of perfect TiO_2, the band gap of electronic forbidden band about 2.16 eV from 0~2 eV [30-32]. Therefore, Pd doping has enhanced the conductivity of perfect TiO_2 by introducing impurity levels around the Fermi level. For C_6H_7N and C_7H_9N adsorption shown in Figure 4(b) and 4(c), The

band structures below -2 eV and above 0 eV are almost the same with that of Pd-TiO_2. However, part of band level is distributed from 0~2 eV when C_6H_7N and C_7H_9N adsorb on the surface of Pd-TiO_2. The impurity levels greatly reduce the transition energy from low level to high level. As a consequence, the conductivity of C_6H_7N and C_7H_9N adsorption system is higher than that of Pd-TiO_2. This conclusion is consistent with the result of DOS analysis above.

Molecular orbital theory is an effective approximation method to deal with the molecular structure with two or more atoms. Molecular orbital was calculated to further verify the conclusion received by DOS analysis. Figure 5 show the orbital distribution of the Highest Occupied Molecular Orbital (HOMO) and the lowest occupied molecular orbital (LUMO). And Table 2 presents the corresponding value of HOMO, LUMO and energy gap (E_g). It is found that the values of E_g for Pd-TiO_2 and gas adsorbed Pd-TiO_2 are small, signifying their good conductivity.

For Pd-TiO_2 shown in Figure 5(a1) and 5(a2) and Table 2, the HOMO mainly locates around Pd atom doping site. And the LUMO mainly locates around the Ti atoms, including a small part on the surface and a main part in the interior of TiO_2. Although the distribution location of HOMO and LUMO are not completely overlap, but the small energy gap (1.06 eV) can still ensure the electron transition from HOMO to LUMO.

For C_6H_7N molecule adsorption shown in Figure 5 (b1) and 5(b2) and Table 2, the value of HOMO and LUMO overall increase with energy gap of 0.05 eV. The HOMO is mainly distributed around Pd and N atoms except a small part around C atoms of C_6H_7N molecule and Ti atom of TiO_2. And the LUMO nearly not occurs on the surface of C_6H_7N molecule. But it significantly increases around Pd comparing with that before C_6H_7N adsorption without obvious change on the other site of TiO_2. The increased distribution location of HOMO and HOMO will enhance the conductivity of adsorption system.

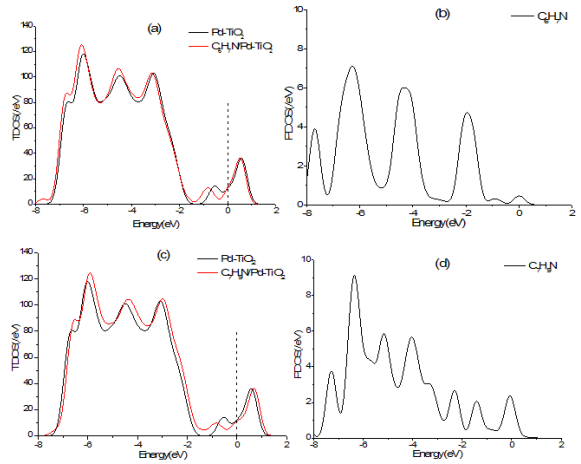

Figure 3: The TDOS of the adsorption systems and the PDOS of adsorbed gas molecules. Dash line presents the Fermi level.

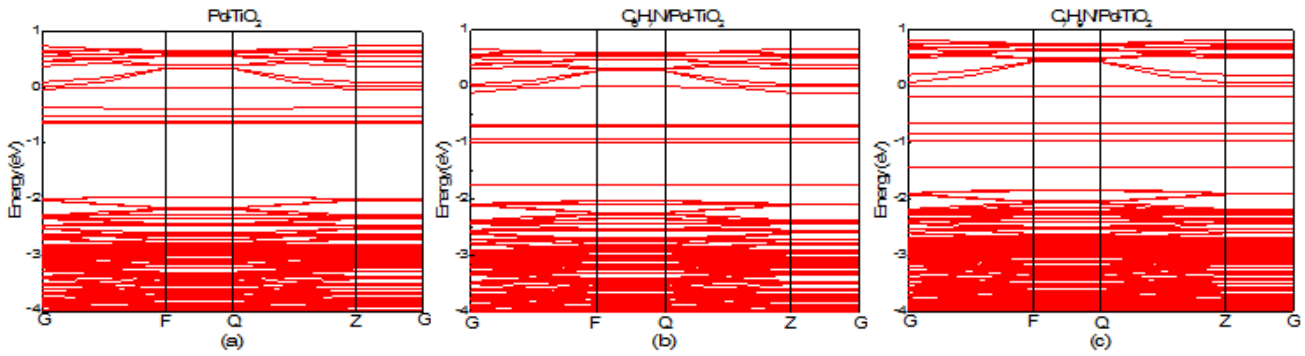

Figure 4: The band structures of Pd-TiO_2 and gas adsorbed Pd-TiO_2. (a) Electronic forbidden band exists in valence band rang -2~-1 eV, (b) The Electronic forbidden band structures below -2 eV and (c) The Electronic forbidden band structures above 0 eV.

System	E_{HOMO}/eV	E_{LUMO}/eV	E_g/eV
Pd-TiO_2	-5.65	-5.59	0.06
C_6H_7N/Pd-TiO_2	-5.49	-5.44	0.05
C_6H_7N/Pd-TiO_2	-5.63	-5.55	0.08

Table 2: The HOMO, LUMO energy and HOMO–LUMO energy gap of C_6H_7N and C_7H_9N adsorption system.

For C_7H_9N adsorption shown in Figure 5 (c1) and 5(c2) and Table 2, the value of HOMO and LUMO is almost the same with that before gas adsorption with energy gap of 0.08 eV. Except of the HOMO located on Pd atom, it also largely distributes around C atom of gas molecule. Therefore, the electrons in HOMO can freely transit between Pd-TiO_2 and C_7H_9N molecule. Because of the long interaction distance and weak adsorption energy between Pd-TiO_2 and C_7H_9N molecule, C_7H_9N adsorption causes little change to the distribution of LUMO on Pd-TiO_2, and brings no distribution on gas molecule. Therefore, the conductivity of C_7H_9N adsorption system increases due to the increase of HOMO distribution.

Conclusion

The first-principles calculation has been applied to analyse the adsorption property of typical lung cancer volatile organic compounds:

C_6H_7N and C_7H_9N on Pd-TiO_2 surface based on DFT theory. Various gas adsorptions structures have been calculated to get obtain the most stable structure shown in this study. Due to the high chemical activity of Pd atoms, it acts as the active site to adsorb gas molecules. C_6H_7N adsorbs by the interaction between Pd atom and N atom of amidogen. And C_7H_9N interacts with Pd atom by H atom of benzene ring. The adsorption energy of C_7H_9N is distantly less that of C_6H_7N because of it larger adsorption distance. And there is little charge transfer in the adsorption process for both of the gas molecules. The physisorption between Pd-TiO_2 and gas molecules (C_6H_7N and C_7H_9N) ensures the good anti-poisoning ability of gas sensors based on Pd-doped TiO_2 material.

According to the analysis of DOS, both of the gas molecules adsorption increases the DOS near Fermi level. And the band structure analysis shows that this gas molecules adsorption introduce new impurity levels around the Fermi level. In addition, gas molecules adsorption makes contribution to increase of the HOMO and LUMO distribution area. Considering the change of DOS, band structure and molecular structure, we conclude that C_6H_7N and C_7H_9N adsorption will increase the conductivity of adsorption system.

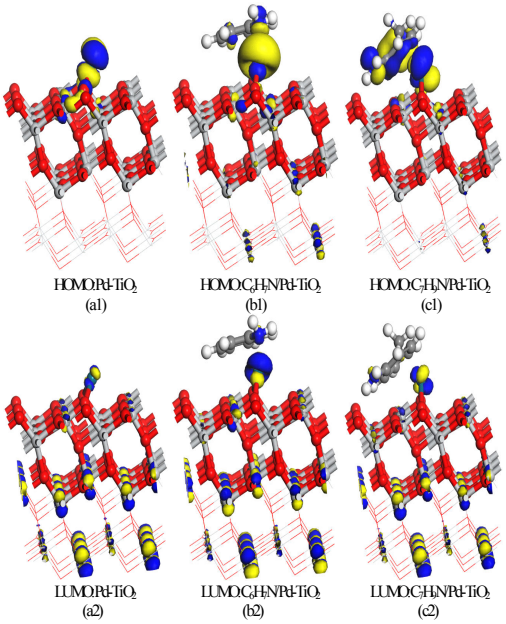

Figure 5: The HOMO and LUMO orbitals on Pd-SWCNTs and molecule-Pd-SWCNTs

Author Contributions

Qianqian Wan developed the analytical model, and performed simulations with Materials Studio. Xiaoxing Zhang generated the basic idea and its application, and supervised the simulation work. All authors collaborated actively in the writing process.

References

1. Siegel RL, Miller KD, Jemal A (2016) Cancer statistics, 2016. CA Cancer J Clin 66: 7-30.
2. Torre LA, Siegel RL, Jemal A (2016) Lung cancer statistics. Lung cancer and personalized medicine: current knowledge and therapies. Springer, Cham 1(Eds) 1-19.
3. Prescott E, Grønbaek M, Becker U, Sørensen TI (1999) Alcohol intake and the risk of lung cancer: influence of type of alcoholic beverage. Am J Epidemiol 149: 463-470.
4. Peto R, Lopez AD, Boreham J, Thun M, Heath C (1994) Mortality from smoking in developed countries 1950-2000. Indirect estimates from national statistics, in, Oxford, New York, Tokyo: Oxford University Press.
5. Luo J, Hendryx M (2011) Environmental carcinogen releases and lung cancer mortality in rural-urban areas of the United States. J Rural Health 27: 342-349.
6. Beeson WL, Abbey DE, Knutsen SF (1998) Long-term concentrations of ambient air pollutants and incident lung cancer in California adults: results from the AHSMOG study. Adventist Health Study on Smog. Environ Health Perspect 106: 813-823.
7. Soheylizad M, Khazaei S, Rezaeian S (2016) Relation between lung cancer incidence and mortality rates with human development index and its components: a global ecological study. Iran J Cancer Prev 9: e5310.
8. Zheng R, Zeng H, Zuo T, Zhang S, Qiao Y, et al. (2016) Lung cancer incidence and mortality in China, 2011. Thorac Cancer 7: 94-99.
9. Atkins GT, Kim T, Munson J (2017) Residence in rural areas of the United States and lung cancer mortality: disease incidence, Treatment Disparities and Stage Specific Survival. Ann Am Thorac Soc 14: 403-411.
10. Devesa SS, Bray F, Vizcaino AP, Parkin DM (2010) International lung cancer trends by histologic type: Male:Female differences diminishing and adenocarcinoma rates rising. Int J Cancer 117: 294-299.
11. Xu ZY, Jin CJ, Shen DY (2007) Clinical study on treatment of advanced non-small-cell lung cancer with Chinese herbal medicine in different stages combined with chemotherapy. Zhongguo Zhong Xi Yi Jie He Za Zhi 27: 874-878.
12. Makrilia N, Strimpakos AS, Gkiozos I, Syrigos KN (2012) Clinical characteristics, diagnosis, treatment, and prognosis in lung cancer patients under the age of 45. Liver Transpl 18: 1209-1216.
13. Hopwood P, Stephens RJ (1995) Symptoms at presentation for treatment in patients with lung cancer: implications for the evaluation of palliative treatment. The Medical Research Council (MRC) Lung Cancer Working Party. Br J Cancer 71: 633-636.
14. Sakumura Y, Koyama Y, Tokutake H, Hida T, Sato K, et al. (2017) Diagnosis by volatile organic compounds in exhaled breath from lung cancer patients using support vector machine algorithm. Sensors (Basel) 17: 287.
15. Byun HG, Yu JB, Jeon JY, Lee SY, Huh JS, et al. (2014) Exhaled breath analysis for lung diseases based on sensors array system. Sens Letters 12: 6-7.
16. Phillips M, Gleeson K, Hughes JM, Greenberg J, Cataneo RN (1999) Volatile organic compounds in breath as markers of lung cancer: a cross-sectional study. Lancet 353: 1930-1933.
17. Arshak K, Moore E, Lyons GM, Harris J, Clifford S (2004) A review of gas sensors employed in electronic nose applications. Sens Review 24: 181-198.
18. Cheng JP, Wang J, Li QQ, Liu HG, Li Y (2016) A review of recent developments in tin dioxide composites for gas sensing application. J Ind Eng Chem 44: 1-22.
19. Wang C, Yin L, Zhang L, Qi Y, Lun N, et al. (2010) Large scale synthesis and gas-sensing properties of anatase TiO2 three-dimensional hierarchical nanostructures. Langmuir 26: 12841-12848.
20. Lu HF, Li F, Liu G, Chen ZG, Wang DW, et al. (2008) Amorphous TiO(2) nanotube arrays for low-temperature oxygen sensors. Nanotechnology 19: 405504.
21. Meng D, Yamazaki T, Kikuta T (2014) Preparation and gas sensing properties of undoped and Pd-doped TiO2 nanowires. Sens Actuators B Chem 190: 838-843.

22. Lü Y, Ling YH, Ma J, Ren FJ, Xu JN (2010) Pd doped TiO2 nanotube arrays: preparation and hydrogen-sensing performance. Chinese J Inorg Chem 26: 627-632.
23. Mukhopadhyay AK (2014) Improvement in ammonia sensing characteristics of titanium dioxide(TiO2) thin film by palladium(Pd) doping. Proceedings of International Conference on Control, Instrumentation, Energy and Communication, 2014 pp. 91-95.
24. An W, Wu AX, Zeng XC (2008) Adsorption of O2, H2, CO, NH3, and NO2 on ZnO Nanotube: A density functional theory study. J Phys Chem C 112: 5747-5755.
25. Zhang X, Chen Q, Hu W, Zhang J (2015) Adsorptions of SO2, SOF2, and SO2F2 on Pt-modified anatase (1 0 1) surface: Sensing mechanism study. Appl Surf Sci 353: 662-669.
26. Zhang X, Gui Y, Dai Z (2014) A simulation of Pd-doped SWCNTs used to detect SF6 decomposition components under partial discharge. Appl Surf Sci 315: 196-202.
27. Zhang X, Dong X, Gui Y (2016) Theoretical and experimental study on competitive adsorption of SF6 decomposed components on Au-modified anatase (101) surface. Appl Surf Sci 387: 437-445.
28. Mulliken RS (1955) Electronic population analysis on LCAO-MO molecular wave functions. IV. Bonding and antibonding in LCAO and valence bond theories. J Chem Phys 23: 2343-2346.
29. Mulliken RS (1955) Electronic population analysis on LCAO–MO molecular wave functions. II. Overlap populations, bond orders, and covalent bond energies. J Chem Phys 23: 1841-1846.
30. Zhang X, Chen Q, Hu W, Zhang J (2013) A DFT study of SF6 decomposed gas adsorption on an anatase (1 0 1) surface. Appl Surf Sci 286: 47-53.
31. Long R, Dai Y, Meng G, Huang B (2009) Energetic and electronic properties of X- (Si, Ge, Sn, Pb) doped TiO2 from first-principles. Phys Chem Chem Phys 11: 8165-8172.
32. Yen CC, Wang DY, Chang LS, Han CS (2011) Characterization and photocatalytic activity of Fe- and N-co-deposited TiO 2 and first-principles study for electronic structure. J Solid State Chem 184: 2053-2060.